Inorganic Chemistry

Article

pubs.acs.org/IC

Homologous Series of Rare-Earth Zinc Arsenides $RE\mathrm{Zn}_{2-x}\mathrm{As}_2{\cdot}n(RE\mathrm{As})$ (RE = La–Nd, Sm; n = 3, 4, 5, 6)

Xinsong Lin and Arthur Mar*

Department of Chemistry, University of Alberta, Edmonton, Alberta, Canada T6G 2G2

Supporting Information

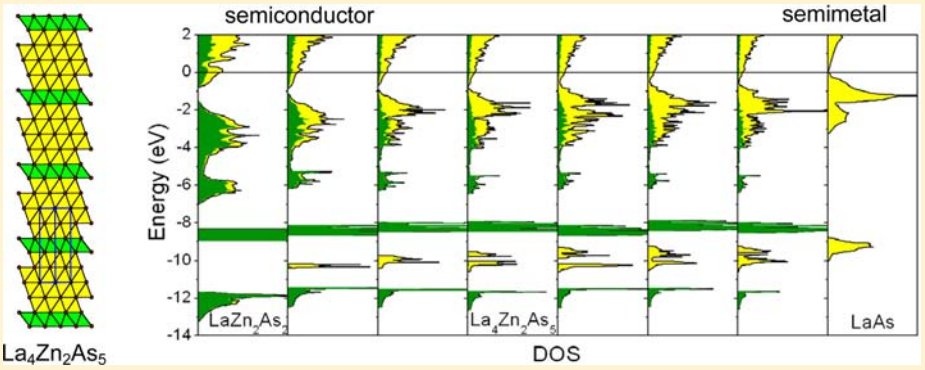

ABSTRACT: Four series of ternary rare-earth zinc arsenides have been prepared by reaction of the elements at 750 °C: $RE_4\mathrm{Zn}_{2-x}\mathrm{As}_5$ forming for RE = La–Nd, Sm; and $RE_5\mathrm{Zn}_{2-x}\mathrm{As}_6$, $RE_6\mathrm{Zn}_{2-x}\mathrm{As}_7$, $RE_7\mathrm{Zn}_{2-x}\mathrm{As}_8$ forming for RE = Ce, Pr, Nd, Sm. They crystallize in trigonal structure types in space group $P\bar{3}m1$ with Z = 1 for $RE_4\mathrm{Zn}_{2-x}\mathrm{As}_5$ and $RE_7\mathrm{Zn}_{2-x}\mathrm{As}_8$, or space group $R\bar{3}m1$ with Z = 3 for $RE_5\mathrm{Zn}_{2-x}\mathrm{As}_6$ and $RE_6\mathrm{Zn}_{2-x}\mathrm{As}_7$. Through the structural principle of intergrowing rocksalt-type [REAs] slabs of variable thickness within a parent $\mathrm{CaAl_2Si_2}$-type structure containing Zn-deficient [$\mathrm{Zn}_{2-x}\mathrm{As}_2$] slabs built from edge-sharing Zn-centered tetrahedra, these ternary arsenides belong to a homologous series with the formulation $RE\mathrm{Zn}_{2-x}\mathrm{As}_2{\cdot}n(RE\mathrm{As})$ (n = 3, 4, 5, 6). Quaternary derivatives $\mathrm{Ce_4(Mn,Zn)}_{2-x}\mathrm{As}_5$ and $\mathrm{Ce_6(Mn,Zn)}_{2-x}\mathrm{As}_7$ were also obtained in which Mn partially substitutes for Zn. Band structure calculations predict that the electronic properties can be gradually modified from semiconducting to semimetallic behavior as more [REAs] slabs are introduced.

INTRODUCTION

Ternary and quaternary arsenides form an emerging class of solid-state materials that have attracted wide attention for their diverse structures and properties, including the recent discovery of superconductivity in $\mathrm{BaFe_2As_2}$ and related compounds.[1−3] Our own efforts have focused on arsenides in combination with electropositive elements (alkali, alkaline-earth, and rare-earth metals) and transition elements.[4−12] The zinc-containing systems are particularly rich, giving rise to complex structures such as those of $\mathrm{K_2Zn_5As_4}$ and $\mathrm{Sr_2Zn_2As_3}$.[7,9] Investigation of ternary RE–Zn–As systems (where RE = rare-earth metal) has led to discovery of many new phases: $RE\mathrm{Zn}_{0.67}\mathrm{As}_2$,[5,13] $RE_{0.67}\mathrm{Zn_2As_2}$,[14] $RE\mathrm{Zn_3As_3}$ (RE = La–Nd, Sm);[6] $RE\mathrm{Zn_2As_3}$ (RE = La–Pr);[11] $RE\mathrm{Zn_2As_2}$ (RE = Eu, Yb);[15−17] $\mathrm{Eu_2Zn_2As_3}$;[7] and $\mathrm{Eu_{11}Zn_6As_{12}}$.[18]

To make sense of the structural chemistry of these arsenides, it has been helpful to identify the $\mathrm{CaAl_2Si_2}$-type structure as a prototype from which other structures can be derived and new compounds can be targeted. The $\mathrm{CaAl_2Si_2}$-type structure can be regarded as a trigonal version of the more common tetragonal $\mathrm{ThCr_2Si_2}$-type structure, found in $\mathrm{BaFe_2As_2}$; both types contain [M_2X_2] slabs formed from edge-sharing metal-centered tetrahedra.[19−22] For example, the $\mathrm{CaAl_2Si_2}$-type structure of $\mathrm{EuZn_2As_2}$ can be retained when divalent Eu is substituted by a trivalent RE element to give $RE_{0.67}\mathrm{Zn_2As_2}$, which is deficient in RE to preserve charge balance.[14] A fully stoichiometric formula is recovered if one of the divalent Zn atoms is replaced by a monovalent Cu atom in $RE\mathrm{CuZnAs_2}$.[23] A different aliovalent substitution leads to alkali-metal containing compounds such as $\mathrm{NaZn}_{1.5}Tt_{0.5}\mathrm{As_2}$ (Tt = Si, Ge).[12] The [$\mathrm{Zn_2As_2}$] slabs in $\mathrm{EuZn_2As_2}$ can also be interrupted with fragments of a hypothetical "EuAs" structure containing $\mathrm{As_2}$ dimers, resulting in $\mathrm{Eu_2Zn_2As_3}$ ($\mathrm{Ba_2Cd_2Sb_3}$-type structure).[7] Finally, it is possible to imagine that such [$\mathrm{Zn_2As_2}$] slabs can intergrow with other types of slabs in various stacking sequences, as long as the trigonal symmetry is maintained, similar to what has been found in the corresponding phosphides.[24−27]

We report here the preparation of four new series of ternary rare-earth zinc arsenides, $RE_4\mathrm{Zn}_{2-x}\mathrm{As}_5$, $RE_5\mathrm{Zn}_{2-x}\mathrm{As}_6$, $RE_6\mathrm{Zn}_{2-x}\mathrm{As}_7$, and $RE_7\mathrm{Zn}_{2-x}\mathrm{As}_8$ (RE = La–Nd, Sm), which belong to a homologous series with the general formula $RE\mathrm{Zn}_{2-x}\mathrm{As}_2{\cdot}n(RE\mathrm{As})$ (n = 3, 4, 5, 6). This formula reflects the intergrowth of rocksalt-type slabs [REAs] of variable thickness

Received: April 15, 2013
Published: May 28, 2013

   dx.doi.org/10.1021/ic400933v | Inorg. Chem. 2013, 52, 7261−7270

between defect [$Zn_{2-x}As_2$] slabs in the parent $CaAl_2Si_2$-type structure. Partial substitution of Mn for Zn is also possible, resulting in quaternary derivatives $RE(Mn,Zn)_{2-x}As_2{\cdot}n(REAs)$. The characterization of these structures, some of which have very long unit cells, suggests that they may form part of a larger family of infinitely adaptive structures, for which few examples are known.[28] Band structure calculations were performed to identify trends in the electronic structure as the number of rocksalt-type slabs is increased.

EXPERIMENTAL SECTION

Synthesis. Starting materials were freshly filed *RE* pieces (*RE* = La−Nd, Sm; 99.9%, Hefa), Zn shot (99.99%, Aldrich), and As lumps (99.999%, Alfa-Aesar). Mixtures of the elements were combined on a 0.3-g scale in stoichiometric ratios corresponding to the idealized formulas $RE_4Zn_2As_5$, $RE_5Zn_2As_6$, $RE_6Zn_2As_7$, and $RE_7Zn_2As_8$ belonging to the homologous Zn-deficient series $REZn_{2-x}As_2{\cdot}n(REAs)$ (n = 3, 4, 5, 6). The mixtures were loaded into fused-silica tubes which were evacuated and sealed. The tubes were heated at 500 °C for 2 d, heated to 750 °C over 20 h, held at this temperature for 7 d, and then cooled to room temperature over 2 d. The products were analyzed by powder X-ray diffraction (XRD) patterns collected on an Inel diffractometer equipped with a curved position-sensitive detector (CPS 120) and a Cu $K\alpha_1$ radiation source. The title compounds generally constituted the major phase of the product (Supporting Information, Figures S1−S4). Completely homogeneous samples were difficult to obtain because of the high volatility of elemental Zn as well as its binary arsenides, which tended to sublimate to the opposite ends of the fused-silica tubes. For a fixed *RE*:As molar ratio (n+1: n+2) used in the synthesis, the powder XRD patterns did not reveal peak broadening or splitting, which would have indicated simultaneous formation of more than one ternary arsenide phase belonging to the homologous series. The unit cell parameters refined from the powder XRD patterns are listed in Table 1. All four series could be prepared for *RE* = Ce, Pr, Nd, Sm, but only the $RE_4Zn_{2-x}As_5$ series was found to form an additional La member. Attempts made to extend the *RE* substitution beyond Sm were unsuccessful under the conditions indicated above. In the course of experiments to investigate substitution of Zn with other transition metals in a different ternary arsenide phase $REZn_3As_3$,[6] crystals of the quaternary Mn-containing derivatives $Ce_4(Mn,Zn)_{2-x}As_5$ and $Ce_6(Mn,Zn)_{2-x}As_7$ were obtained and identified to belong to the homologous series presented here.

Table 1. Cell Parameters for $REZn_{2-x}As_2{\cdot}n(REAs)$ (*RE* = La−Nd, Sm; n = 3, 4, 5, 6)[a]

compound	a (Å)	c (Å)	V (Å^3)
$La_4Zn_{2-x}As_5$	4.3172(2)	17.711(2)	285.88(2)
$Ce_4Zn_{2-x}As_5$	4.2666(5)	17.579(3)	277.13(4)
$Pr_4Zn_{2-x}As_5$	4.2619(2)	17.362(2)	273.11(2)
$Nd_4Zn_{2-x}As_5$	4.2437(2)	17.051(1)	265.93(2)
$Sm_4Zn_{2-x}As_5$	4.1926(2)	16.804(1)	255.82(2)
$Ce_5Zn_{2-x}As_6$	4.2630(1)	62.861(3)	989.35(6)
$Pr_5Zn_{2-x}As_6$	4.2426(1)	62.467(3)	973.73(6)
$Nd_5Zn_{2-x}As_6$	4.2184(1)	61.953(3)	954.76(6)
$Sm_5Zn_{2-x}As_6$	4.1722(1)	61.201(3)	922.61(6)
$Ce_6Zn_{2-x}As_7$	4.2672(1)	73.583(3)	1160.38(7)
$Pr_6Zn_{2-x}As_7$	4.2456(1)	72.922(3)	1138.32(7)
$Nd_6Zn_{2-x}As_7$	4.2278(1)	72.492(3)	1122.15(7)
$Sm_6Zn_{2-x}As_7$	4.1733(1)	71.678(3)	1081.17(6)
$Ce_7Zn_{2-x}As_8$	4.2675(1)	28.018(1)	441.88(3)
$Pr_7Zn_{2-x}As_8$	4.2411(1)	27.815(1)	433.28(2)
$Nd_7Zn_{2-x}As_8$	4.2283(1)	27.621(1)	427.68(2)
$Sm_7Zn_{2-x}As_8$	4.1704(1)	27.293(1)	411.09(2)

[a]Powder samples obtained by reaction of the elements at 750 °C.

The synthetic procedure described above did not normally lead to sufficiently large crystals for structure determination. To promote crystal growth, the as-prepared samples were reheated at 800 °C for 2 d, heated to 1050 °C over 20 h, held at this temperature for 7 d, slowly cooled to 500 °C at a rate of 3 °C/h, and cooled to room temperature over 2 d. The compositions of crystals used for the single-crystal diffraction experiments below were determined by energy-dispersive X-ray (EDX) analysis with a JEOL JSM-6010LA scanning electron microscope. Several points on individual crystals were analyzed with acquisition times of 30 s each. Although most of the results agree acceptably with expectations (Supporting Information, Table S1), larger deviations were noted in some samples probably because the surfaces were irregular.

Structure Determination. Representative *RE* members from each of the four series $REZn_{2-x}As_2{\cdot}n(REAs)$ (n = 3, 4, 5, 6), as well as two quaternary derivatives $Ce_4(Mn,Zn)_{2-x}As_5$ and $Ce_6(Mn,Zn)_{2-x}As_7$, were chosen for structure determination. Single-crystal intensity data were collected on a Bruker PLATFORM diffractometer equipped with a SMART APEX II CCD detector and a Mo $K\alpha$ radiation source, using ω scans at 5−7 different ϕ angles with a frame width of 0.3° and an exposure time of 12−15 s per frame. Face-indexed numerical absorption corrections were applied. Structure solution and refinement were carried out with use of the SHELXTL (version 6.12) program package.[29] Crystal data and further experimental details are given in Table 2.

Within the $RE_4Zn_{2-x}As_5$ series, a crystal of the La member and two crystals of the Pr member (from different batches) were examined. The trigonal centrosymmetric space group $P\bar{3}m1$ was chosen on the basis of Laue symmetry, systematic absences, and intensity statistics. Direct methods led to a structural model containing 6 atomic sites and corresponding to an ideal formula of "$RE_4Zn_2As_5$". Refinements based on this model led to somewhat elevated displacement parameters for the Zn site (~0.02−0.03 Å^2) relative to the other sites (~0.01 Å^2), suggesting partial occupancy. When refined, the Zn occupancy converged to ~0.8−0.9 and the displacement parameter was reduced to more reasonable values, resulting in the formulas $La_4Zn_{1.66(1)}As_5$, $Pr_4Zn_{1.68(1)}As_5$, and $Pr_4Zn_{1.80(1)}As_5$. Because the crystals were obtained from the loading compositions $RE_4Zn_2As_5$ (i.e., with an excess of Zn), we assume that these formulas correspond to the maximum Zn content possible. With the understanding that refinements of occupancies are sensitive to other factors (such as absorption corrections), the similarity of the refined formulas for the two Pr crystals implies that a significant homogeneity range in Zn is unlikely.

Structure determinations for higher members (n = 4, 5, 6) of the homologous series proceeded in a similar fashion as above. All exhibited trigonal symmetry, with the c-parameters being very long for the n = 4 and 5 members (up to 73 Å for the latter). Structural models were proposed by direct methods for $Pr_5Zn_{2-x}As_5$ and $Nd_6Zn_{2-x}As_6$ in space group $R\bar{3}m1$, and for $Pr_7Zn_{2-x}As_8$ in space group $P\bar{3}m1$. Refinements of these models revealed again that the Zn sites were partially occupied (~0.8−0.9). In $Nd_6Zn_{2-x}As_8$, there remained residual electron density (~16 e$^-$/Å^2) in the difference map which was assigned to be a second Zn site (labeled Zn2). Because this site is located at unphysical distances to the existing Zn site (now labeled Zn1) at ~0.9 Å and to the As1 site at ~1.7 Å, constraints were applied so that the occupancies of the Zn2 and As1 sites must sum to unity while the occupancy of the main Zn1 site was freely refined, and the displacement parameters for the Zn1 and Zn2 site were set to be isotropic and equal. The occupancies converged to 0.74(1) for Zn1, 0.09(1) for Zn2, and 0.91(1) for As1, corresponding to the formula $Nd_6Zn_{1.65(2)}As_{6.83(1)}$. Although $Pr_5Zn_{2-x}As_5$ and $Pr_7Zn_{2-x}As_8$ suffered from similar problems albeit to a lesser extent, refinements including this extra site were unstable. With only one Zn site present in the structural models, refinement of its occupancy led to the formulas $Pr_5Zn_{1.73(2)}As_6$ and $Pr_7Zn_{1.76(2)}As_8$.

The quaternary arsenides $Ce_4(Mn,Zn)_{2-x}As_5$ and $Ce_6(Mn,Zn)_{2-x}As_7$ were found to be isostructural to $RE_4Zn_{2-x}As_5$ (space group $P\bar{3}m1$) and $RE_6Zn_{2-x}As_7$ (space group $R\bar{3}m1$), respectively, but with Mn atoms disordering within the Zn site. This site was assumed to be partially occupied with a mixture of Mn and Zn

dx.doi.org/10.1021/ic400933v | Inorg. Chem. 2013, 52, 7261−7270

Table 2. Crystallographic Data for $RE Zn_{2-x}As_2 \cdot n(RE As)$ and $RE(Mn,Zn)_{2-x}As_2 \cdot n(RE As)$ (RE = La–Nd, Sm; n = 3, 4, 5, 6)

formula	$La_4Zn_{1.66(1)}As_5$	$Ce_4Mn_{0.6}Zn_{1.2}As_5$	$Pr_4Zn_{1.68(1)}As_5$	$Pr_4Zn_{1.80(1)}As_5$
formula mass (amu)	1039.41	1043.32	1048.06	1055.91
space group	$P\bar{3}m1$ (No. 164)	$P\bar{3}m1$ (No. 164)	$P\bar{3}m1$ (No. 164)	$P\bar{3}m1$ (No. 164)
a (Å)	4.315(2)	4.288(6)	4.245(2)	4.2409(7)
c (Å)	17.692(10)	17.59(3)	17.385(17)	17.390(3)
V (Å^3)	285.2(3)	280.1(7)	271.4(3)	270.86(8)
Z	1	1	1	1
ρ_{calcd} (g cm^{-3})	6.051	6.185	6.414	6.473
T (K)	296(2)	296(2)	296(2)	296(2)
crystal dimensions (mm)	0.04 × 0.03 × 0.03	0.05 × 0.04 × 0.03	0.04 × 0.04 × 0.03	0.03 × 0.03 × 0.03
radiation	graphite monochromated Mo $K\alpha$, λ = 0.71073 Å			
μ(Mo $K\alpha$) (mm^{-1})	32.43	33.59	36.32	36.64
transmission factors	0.425–0.534	0.365–0.547	0.278–0.482	0.563–0.678
2θ limits	4.60–66.44°	4.64–66.32°	4.68–66.46°	4.68–66.50°
data collected	$-6 \le h \le 6$	$-6 \le h \le 6$	$-6 \le h \le 6$	$-6 \le h \le 6$
	$-6 \le k \le 6$	$-6 \le k \le 6$	$-6 \le k \le 6$	$-6 \le k \le 6$
	$-26 \le l \le 26$	$-26 \le l \le 27$	$-26 \le l \le 26$	$-26 \le l \le 25$
no. of data collected	4020	3873	3792	3882
no. of unique data, including $F_o^2 < 0$	499 (R_{int} = 0.045)	489 (R_{int} = 0.060)	475 (R_{int} = 0.025)	479 (R_{int} = 0.039)
no. of unique data, with $F_o^2 > 2\sigma(F_o^2)$	395	385	424	392
no. of variables	20	19	20	20
$R(F)$ for $F_o^2 > 2\sigma(F_o^2)$[a]	0.022	0.031	0.017	0.026
$R_w(F_o^2)$[b]	0.048	0.098	0.038	0.066
goodness of fit	1.04	1.09	1.06	1.12
$(\Delta\rho)_{max}$, $(\Delta\rho)_{min}$ (e Å^{-3})	1.69, −1.22	5.04, −4.24	1.55, −1.48	3.98, −1.38

formula	$Pr_5Zn_{1.73(2)}As_6$	$Ce_6Mn_{0.4}Zn_{1.3}As_7$	$Nd_6Zn_{1.65(2)}As_{6.83(1)}$	$Pr_7Zn_{1.76(2)}As_8$
formula mass (amu)	1268.47	1472.46	1486.34	1703.40
space group	$R\bar{3}m1$ (No. 166)	$R\bar{3}m1$ (No. 166)	$R\bar{3}m1$ (No. 166)	$P\bar{3}m1$ (No. 164)
a (Å)	4.246(3)	4.2821(8)	4.2283(14)	4.254(7)
c (Å)	62.49(5)	73.620(14)	72.58(2)	27.82(5)
V (Å^3)	976(1)	1169.1(4)	1123.8(6)	436(1)
Z	3	3	3	1
ρ_{calcd} (g cm^{-3})	6.475	6.274	6.588	6.487
T (K)	296(2)	296(2)	296(2)	296(2)
crystal dimensions (mm)	0.03 × 0.03 × 0.02	0.05 × 0.03 × 0.02	0.03 × 0.03 × 0.02	0.03 × 0.03 × 0.02
radiation	graphite monochromated Mo $K\alpha$, λ = 0.71073 Å			
μ(Mo $K\alpha$) (mm^{-1})	36.61	34.11	37.94	36.60
transmission factors	0.429–0.585	0.214–0.359	0.328–0.506	0.464–0.569
2θ limits	3.92–66.30°	3.32–66.48°	3.36–66.46°	4.40–66.52°
data collected	$-6 \le h \le 6$	$-6 \le h \le 6$	$-6 \le h \le 6$	$-6 \le h \le 6$
	$-6 \le k \le 6$	$-6 \le k \le 6$	$-6 \le k \le 6$	$-6 \le k \le 6$
	$-93 \le l \le 94$	$-111 \le l \le 110$	$-109 \le l \le 109$	$-42 \le l \le 42$
no. of data collected	4681	5613	5276	6105
no. of unique data, including $F_o^2 < 0$	572 (R_{int} = 0.123)	685 (R_{int} = 0.065)	658 (R_{int} = 0.106)	764 (R_{int} = 0.083)
no. of unique data, with $F_o^2 > 2\sigma(F_o^2)$	323	437	358	473
no. of variables	23	25	26	29
$R(F)$ for $F_o^2 > 2\sigma(F_o^2)$[a]	0.036	0.029	0.052	0.038
$R_w(F_o^2)$[b]	0.092	0.072	0.158	0.109
goodness of fit	0.98	1.06	1.02	1.04
$(\Delta\rho)_{max}$, $(\Delta\rho)_{min}$ (e Å^{-3})	6.79, −3.44	5.57, −2.02	9.49, −4.12	5.34, −2.43

[a] $R(F) = \sum||F_o| - |F_c||/\sum|F_o|$. [b] $R_w(F_o^2) = [\sum[w(F_o^2 - F_c^2)^2]/\sum wF_o^4]^{1/2}$; $w^{-1} = [\sigma^2(F_o^2) + (Ap)^2 + Bp]$, where $p = [\max(F_o^2,0) + 2F_c^2]/3$.

atoms in a fixed proportion according to the experimental composition determined by EDX analyses on these crystals (Supporting Information, Table S1), corresponding to the formulas $Ce_4Mn_{0.6}Zn_{1.2}As_5$ and $Ce_6Mn_{0.4}Zn_{1.3}As_7$.

Atomic coordinates for all structures were standardized with use of the program STRUCTURE TIDY.[30] Final values of the positional and displacement parameters are given in Table 3, and selected interatomic distances are given in Table 4. Further data in the form of crystallographic information files (CIFs) are available as Supporting Information or may be obtained from Fachinformationszentrum Karlsruhe, Abt. PROKA, 76344 Eggenstein-Leopoldshafen, Germany (CSD-426021 to 426028).

Band Structure Calculations. Tight-binding linear muffin tin orbital band structure calculations were performed within the local density and atomic spheres approximation with use of the Stuttgart TB-LMTO-ASA program (version 4.7).[31] Fully stoichiometric models $La_4Zn_2As_5$, $La_5Zn_2As_6$, $La_6Zn_2As_7$, and $La_7Zn_2As_8$ were considered subject to these conditions: the cell parameters were taken from the

dx.doi.org/10.1021/ic400933v | Inorg. Chem. 2013, 52, 7261–7270

Table 3. Atomic Coordinates and Equivalent Isotropic Displacement Parameters for $RE\mathrm{Zn}_{2-x}\mathrm{As}_2{\cdot}n(RE\mathrm{As})$ and $RE(\mathrm{Mn,Zn})_{2-x}\mathrm{As}_2{\cdot}n(RE\mathrm{As})$ (RE = La−Nd, Sm; n = 3, 4, 5, 6)

atom	Wyckoff position	occupancy	x	y	z	U_{eq} (Å^2)[a]
			$La_4Zn_{1.66(1)}As_5$			
La1	2*d*	1	1/3	2/3	0.09975(2)	0.0079(1)
La2	2*c*	1	0	0	0.29977(3)	0.0101(1)
Zn	2*d*	0.831(4)	1/3	2/3	0.55099(7)	0.0178(4)
As1	2*d*	1	1/3	2/3	0.40622(4)	0.0106(2)
As2	2*d*	1	1/3	2/3	0.79675(4)	0.0083(2)
As3	1*a*	1	0	0	0	0.0084(2)
			$Ce_4Mn_{0.6}Zn_{1.2}As_5$			
Ce1	2*d*	1	1/3	2/3	0.09925(3)	0.0085(2)
Ce2	2*c*	1	0	0	0.29819(4)	0.0111(2)
M	2*d*	0.29 Mn, 0.58 Zn	1/3	2/3	0.55156(11)	0.0158(4)
As1	2*d*	1	1/3	2/3	0.40475(8)	0.0116(3)
As2	2*d*	1	1/3	2/3	0.79784(6)	0.0092(3)
As3	2*c*	1	0	0	0	0.0098(4)
			$Pr_4Zn_{1.68(1)}As_5$			
Pr1	2*d*	1	1/3	2/3	0.09923(2)	0.0064(1)
Pr2	2*c*	1	0	0	0.29815(2)	0.0088(1)
Zn	2*d*	0.841(4)	1/3	2/3	0.55201(5)	0.0157(3)
As1	2*d*	1	1/3	2/3	0.40398(4)	0.0089(1)
As2	2*d*	1	1/3	2/3	0.79808(3)	0.0070(1)
As3	2*c*	1	0	0	0	0.0068(2)
			$Pr_4Zn_{1.80(1)}As_5$			
Pr1	2*d*	1	1/3	2/3	0.09900(3)	0.0078(2)
Pr2	2*c*	1	0	0	0.29797(3)	0.0091(2)
Zn	2*d*	0.902(5)	1/3	2/3	0.55289(8)	0.0178(4)
As1	2*d*	1	1/3	2/3	0.40462(6)	0.0096(2)
As2	2*d*	1	1/3	2/3	0.79793(5)	0.0075(2)
As3	2*c*	1	0	0	0	0.0082(3)
			$Pr_5Zn_{1.73(2)}As_6$			
Pr1	6*c*	1	0	0	0.27792(2)	0.0104(3)
Pr2	6*c*	1	0	0	0.44433(2)	0.0128(3)
Pr3	3*a*	1	0	0	0	0.0097(3)
Zn	6*c*	0.863(9)	0	0	0.15215(5)	0.0220(9)
As1	6*c*	1	0	0	0.08406(3)	0.0094(4)
As2	6*c*	1	0	0	0.19319(3)	0.0122(4)
As3	6*c*	1	0	0	0.36133(3)	0.0087(3)
			$Ce_6Mn_{0.4}Zn_{1.3}As_7$			
Ce1	6*c*	1	0	0	0.07136(1)	0.0104(2)
Ce2	6*c*	1	0	0	0.30953(1)	0.0107(2)
Ce3	6*c*	1	0	0	0.45218(1)	0.0133(2)
M	6*c*	0.21 Mn, 0.64 Zn	0	0	0.17898(3)	0.0169(4)
As1	6*c*	1	0	0	0.14411(2)	0.0133(3)
As2	6*c*	1	0	0	0.23738(2)	0.0106(3)
As3	6*c*	1	0	0	0.38125(2)	0.0108(3)
As4	3*a*	1	0	0	0	0.0109(4)
			$Nd_6Zn_{1.65(2)}As_{6.83(1)}$			
Nd1	6*c*	1	0	0	0.07125(2)	0.0139(3)
Nd2	6*c*	1	0	0	0.30960(2)	0.0134(3)
Nd3	6*c*	1	0	0	0.45222(2)	0.0190(4)
Zn1	6*c*	0.740(12)	0	0	0.17918(6)	0.024(2)[b]
Zn2	6*c*	0.086(6)	0	0	0.1681(6)	0.024(2)[b]
As1	6*c*	0.914(6)	0	0	0.14380(4)	0.0137(7)
As2	6*c*	1	0	0	0.23755(3)	0.0143(5)
As3	6*c*	1	0	0	0.38119(3)	0.0132(5)
As4	3*a*	1	0	0	0	0.0139(7)
			$Pr_7Zn_{1.76(2)}As_8$			
Pr1	2*d*	1	1/3	2/3	0.24995(3)	0.0098(2)
Pr2	2*d*	1	1/3	2/3	0.87497(3)	0.0098(2)
Pr3	2*c*	1	0	0	0.37525(3)	0.0123(2)
Pr4	1*a*	1	0	0	0	0.0097(3)

dx.doi.org/10.1021/ic400933v | *Inorg. Chem.* 2013, 52, 7261−7270

Table 3. continued

atom	Wyckoff position	occupancy	x	y	z	U_{eq} (Å^2)[a]
			$Pr_7Zn_{1.76(2)}As_8$			
Zn	2*d*	0.879(9)	1/3	2/3	0.53265(9)	0.0237(8)
As1	2*d*	1	1/3	2/3	0.06291(5)	0.0097(3)
As2	2*d*	1	1/3	2/3	0.44056(6)	0.0130(4)
As3	2*d*	1	1/3	2/3	0.68541(5)	0.0099(3)
As4	2*c*	1	0	0	0.18862(5)	0.0090(3)

[a]U_{eq} is defined as one-third of the trace of the orthogonalized U_{ij} tensor. [b]Zn1 and Zn2 atoms in $Nd_6Zn_{1.65(2)}As_{6.83(1)}$ were modeled with isotropic displacement parameters (U_{iso}), constrained to be equal.

Table 4. Interatomic Distances (Å) in $RE Zn_{2-x}As_2 \cdot n(RE As)$ and $RE(Mn,Zn)_{2-x}As_2 \cdot n(RE As)$ (RE = La–Nd, Sm; n = 3, 4, 5, 6)

$La_4Zn_{1.66(1)}As_5$		$Ce_4Mn_{0.6}Zn_{1.2}As_5$	
La1–As3 (×3)	3.053(1)	Ce1–As3 (×3)	3.029(3)
La1–As2 (×3)	3.092(1)	Ce1–As2 (×3)	3.067(3)
La2–As2 (×3)	3.020(1)	Ce2–As2 (×3)	2.997(3)
La2–As1 (×3)	3.123(1)	Ce2–As1 (×3)	3.105(3)
Zn–As1	2.561(2)	*M*–As1	2.582(4)
Zn–As1 (×3)	2.603(1)	*M*–As1 (×3)	2.592(4)
Zn–Zn (×3)	3.076(2)	*M*–*M* (×3)	3.069(4)
$Pr_4Zn_{1.68(1)}As_5$		$Pr_4Zn_{1.80(1)}As_5$	
Pr1–As3 (×3)	2.997(1)	Pr1–As3 (×3)	2.993(1)
Pr1–As2 (×3)	3.032(1)	Pr1–As2 (×3)	3.034(1)
Pr2–As2 (×3)	2.967(1)	Pr2–As2 (×3)	2.963(1)
Pr2–As2 (×3)	3.065(1)	Pr2–As2 (×3)	3.072(1)
Zn–As1 (×3)	2.568(1)	Zn–As1 (×3)	2.558(1)
Zn–As1	2.573(3)	Zn–As1	2.578(2)
Zn–Zn (×3)	3.046(2)	Zn–Zn (×3)	3.062(2)
$Pr_5Zn_{1.73(2)}As_6$		$Ce_6Mn_{0.4}Zn_{1.3}As_7$	
Pr1–As3 (×3)	2.991(2)	Ce1–As3 (×3)	3.015(1)
Pr1–As1 (×3)	3.036(2)	Ce1–As1 (×3)	3.065(1)
Pr2–As1 (×3)	2.974(2)	Ce2–As4 (×3)	3.030(1)
Pr2–As2 (×3)	3.054(2)	Ce2–As3 (×3)	3.044(1)
Pr3–As3 (×6)	3.012(2)	Ce3–As2 (×3)	2.992(1)
Zn–As2 (×3)	2.564(2)	Ce3–As1 (×3)	3.094(1)
Zn–As2	2.565(4)	*M*–As1	2.567(3)
Zn–Zn (×3)	3.050(4)	*M*–As1 (×3)	2.585(1)
		M–*M* (×3)	3.066(3)
$Nd_6Zn_{1.65(2)}As_{6.83(1)}$		$Pr_7Zn_{1.76(2)}As_8$	
Nd1–As3 (×3)	2.974(2)	Pr1–As4 (×3)	2.991(4)
Nd1–As2 (×3)	3.022(2)	Pr1–As3 (×3)	3.044(4)
Nd2–As4 (×3)	2.988(1)	Pr2–As1 (×3)	3.003(4)
Nd2–As3 (×3)	3.004(2)	Pr2–As4 (×3)	3.027(4)
Nd3–As2 (×3)	2.962(2)	Pr3–As3 (×3)	2.980(4)
Nd3–As1 (×3)	3.038(2)	Pr3–As2 (×3)	3.055(4)
Zn1–As1 (×3)	2.554(2)	Pr4–As1 (×6)	3.016(4)
Zn1–As1	2.568(5)	Zn–As2	2.562(5)
Zn1–Zn1 (×3)	3.043(6)	Zn–As2 (×3)	2.567(4)
Zn2–As1 (×3)	2.94(2)	Zn–Zn (×3)	3.055(5)
Zn2–Zn2 (×3)	2.442(2)		

experimental values found for the Ce-containing members, which form for all four series (n = 3, 4, 5, 6); atomic positions were taken from the single-crystal structure refinements; and the *RE* component was chosen to be La, to avoid computational difficulties associated with occupied 4f orbitals. Similarly, the band structure of $CaAl_2Si_2$-type $LaZn_2As_2$ (n = 0) was calculated on the basis of the previously reported structure of $Ce_{0.63}Zn_2As_2$.[14] Models of the hypothetical members $La_2Zn_2As_3$ (n = 1) and $La_3Zn_2As_4$ (n = 2) were constructed to give realistic bond lengths (La–As, 3.1 Å; Zn–As, 2.6 Å). The band structure of rocksalt-type LaAs, in the cubic space group $Fm\bar{3}m$ with a cell parameter of 6.16 Å, was also examined.[32,33] The basis set consisted of La 6s/6p/5d/4f, Zn 4s/4p/3d, and As 4s/4p/4d orbitals, with the La 6p and As 4d orbitals being downfolded. Integrations in reciprocal space were carried out with an improved tetrahedron method over varying *k*-point meshes within the first Brillouin zone depending on the structure.

RESULTS AND DISCUSSION

Reaction of the elements at 750 °C resulted in four new series of ternary arsenides, $RE_4Zn_{2-x}As_5$ (*RE* = La–Nd, Sm), $RE_5Zn_{2-x}As_6$, $RE_6Zn_{2-x}As_7$, and $RE_7Zn_{2-x}As_8$ (*RE* = Ce, Pr, Nd, Sm), which follow the general formula $RE Zn_{2-x}As_2 \cdot n(RE As)$ (n = 3, 4, 5, 6) and adopt trigonal crystal structures. The corresponding Zn-deficient phosphides, $RE Zn_{2-x}P_2 \cdot n(RE P)$ (n = 2, 3, 4), have also been previously reported but are restricted to *RE* = La and Ce.[25−27] The Zn deficiencies in the ternary arsenides as determined from the crystal structure refinements lead to compositions $RE Zn_{1.7-1.8}As_2 \cdot n(RE As)$. The phase relationships in these *RE*–Zn–As systems are complex, being characterized by the occurrence of many ternary phases, some exhibiting several polymorphic modifications. The n = 0 member of the homologous series would have the Zn-deficient formula $RE Zn_{2-x}As_2$ and adopt the trigonal $CaAl_2Si_2$-type structure. However, the experimentally observed phases are actually *RE*-deficient, $RE_{0.67}Zn_2As_2$ (*RE* = La–Nd, Sm),[14] or they are fully stoichiometric when *RE* is divalent, as seen in $EuZn_2As_2$ and $YbZn_2As_2$.[15−17] Further, $RE_{0.67}Zn_2As_2$ has the same composition as $RE Zn_3As_3$, which adopts either a new orthorhombic structure (for *RE* = La) or the $ScAl_3C_3$-type structure (for *RE* = Ce, Pr, Nd, Sm).[6] There do exist Zn-deficient phases $RE Zn_{0.67}As_2$ (*RE* = La–Nd, Sm) but they are derived from a different ideal formula $RE Zn_{1-x}As_2$ and adopt the tetragonal $HfCuSi_2$-type structure.[5,13] The recent discovery of $RE Zn_2As_3$ (*RE* = La–Pr), which is closely related to $RE Zn_{0.67}As_2$ but with thicker PbO-type slabs, suggests the emergence of a separate branch of homologous structures based on stackings of square nets.[11] As the enumeration of the $RE Zn_{2-x}As_2 \cdot n(RE As)$ series is continued, the n = 1 member would have the formula $RE_2Zn_{2-x}As_3$. No such compounds are known for the early *RE* metals, but fully stoichiometric $Eu_2Zn_2As_3$ has been reported with an entirely different monoclinic structure ($Ba_2Cd_2Sb_3$-type).[7] The unknown n = 3 member is predicted to have the formula $RE_3Zn_{2-x}As_4$, and the next member beyond the title compounds, n = 7, would be $RE_8Zn_{2-x}As_9$. We were unsuccessful in attempts to prepare these missing members under the same synthetic conditions as the existing ones.

The ternary arsenides crystallize in either space group $P\bar{3}m1$ with Z = 1 for $RE_4Zn_{2-x}As_5$ and $RE_7Zn_{2-x}As_8$, or space group $R\bar{3}m1$ with Z = 3 for $RE_5Zn_{2-x}As_6$ and $RE_6Zn_{2-x}As_7$. Normalized to the formula unit, the cell volumes within each series gradually decrease as expected on proceeding to the

dx.doi.org/10.1021/ic400933v | Inorg. Chem. 2013, 52, 7261−7270

smaller *RE* metals (Figure 1a). For a fixed *RE*, the cell volume increases by about 53 Å^3 per formula unit on proceeding to

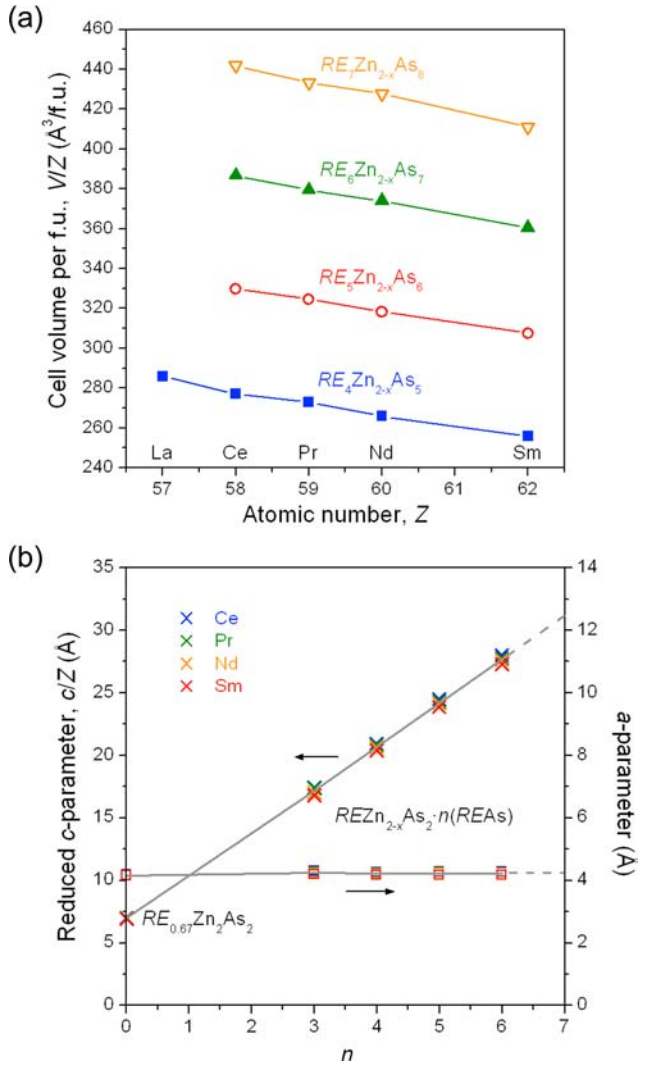

Figure 1. (a) Plot of cell volume per formula unit and (b) plots of cell lengths for $RE\mathrm{Zn}_{2-x}\mathrm{As}_2{\cdot}n(RE\mathrm{As})$. For rhomobohedral structures ($R\bar{3}m1$), the *c*-parameter is divided by 3 to permit comparison to the primitive structures ($P\bar{3}m1$).

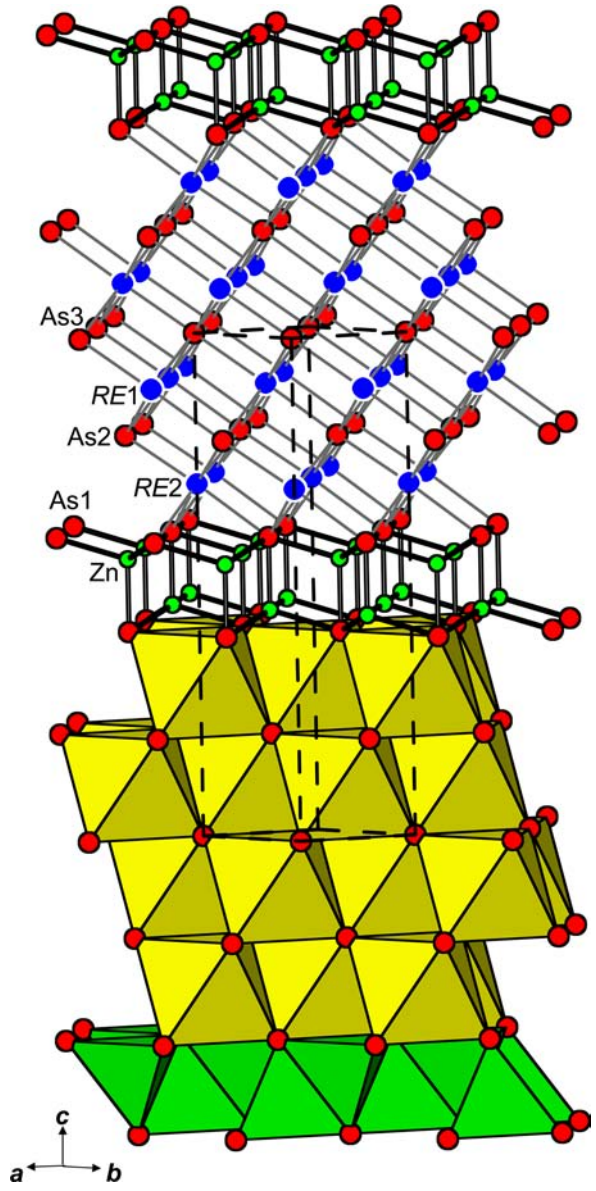

Figure 2. Structure of $RE_4\mathrm{Zn}_{2-x}\mathrm{As}_5$ (*RE* = La−Nd, Sm) highlighting the [*RE*As] slabs built from edge-sharing octahedra (yellow) and [$\mathrm{Zn}_2\mathrm{As}_2$] slabs built from edge-sharing tetrahedra (green).

successively higher members (increasing *n*) of the homologous series. This cell expansion comes about through an elongation of the *c*-parameter by increments of about 3.4 Å (normalized per formula unit) while the *a*-parameter remains relatively constant at about 4.2 Å (Figure 1b).

The crystal structure of $RE_4\mathrm{Zn}_{2-x}\mathrm{As}_5$ (Figure 2) serves as a starting point for the structural description. The As atoms are arranged in close-packed nets which stack in the sequence ABCBC along the *c*-direction. If the formula is idealized to $RE_4\mathrm{Zn}_2\mathrm{As}_5$, the *RE* atoms occupy 4/5 of the octahedral sites and the Zn atoms occupy 1/5 of the tetrahedral sites available between these nets. The *RE*-centered octahedra share edges within the *ab*-plane as well as edges along the *c*-direction to generate quadruple slabs $[RE\mathrm{As}]_4$ that are fragments of the rocksalt structure (NaCl-type). The Zn-centered tetrahedra share edges within the *ab*-plane to generate [$\mathrm{Zn}_2\mathrm{As}_2$] slabs; with the 3-fold rotation axes of these tetrahedra aligned along the *c*-direction, half point up and half point down. These [$\mathrm{Zn}_2\mathrm{As}_2$] slabs are found in the $\mathrm{CaAl}_2\mathrm{Si}_2$-type structure which would be adopted by the simplest member (n = 0) of the homologous series, $RE\mathrm{Zn}_{2-x}\mathrm{As}_2$, which also contains one [*RE*As] slab. The structures of all members of the homologous series $RE\mathrm{Zn}_{2-x}\mathrm{As}_2{\cdot}n(RE\mathrm{As})$ are thus built up from the intergrowth of the $\mathrm{CaAl}_2\mathrm{Si}_2$-type structure with NaCl-type slabs of increasing thickness (Figure 3). Writing the stacking sequences of the As atoms can become very unwieldy, so it is convenient to represent them in Jagodzinski notation to differentiate between nets that are surrounded in hexagonal vs cubic stacking (e.g., *h* = A<u>B</u>A; *c* = A<u>B</u>C).[34] For example, the stacking sequence in $RE_5\mathrm{Zn}_{2-x}\mathrm{As}_6$ is *hhccccc* or h^2c^5. The Ramsdel symbol for this sequence is 21*R*, which emphasizes the repeating number of nets and the lattice type (*H* vs *R*).[34] On the basis of this structural principle of adding [*RE*As] slabs, each with an approximate thickness of 3.4 Å, it becomes possible to predict the structural features of further hypothetical members belonging to the homologous series (Table 5). The

dx.doi.org/10.1021/ic400933v | *Inorg. Chem.* 2013, 52, 7261−7270

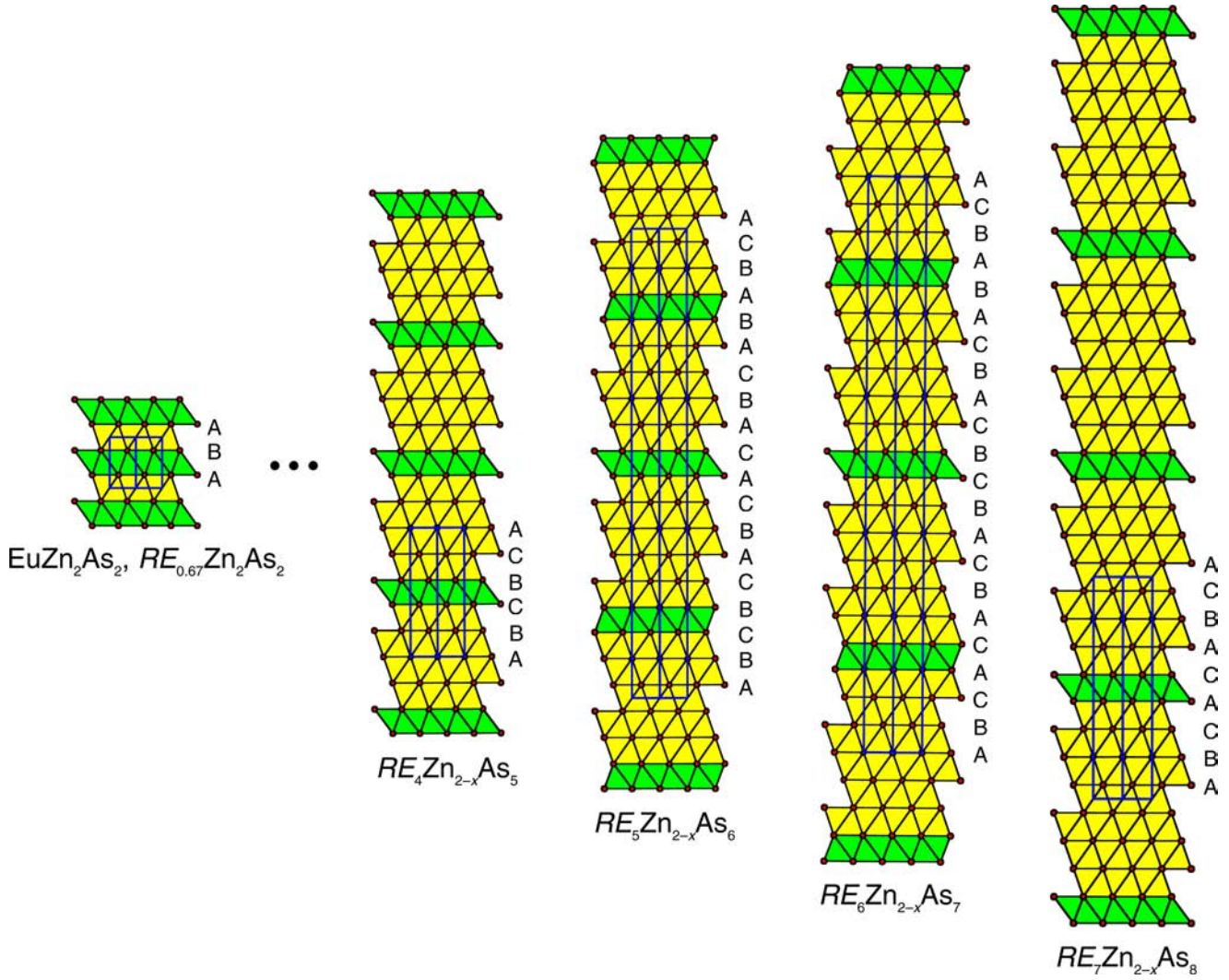

Figure 3. Evolution of structures in the homologous series $RE\mathrm{Zn}_{2-x}\mathrm{As}_2{\cdot}n(RE\mathrm{As})$, shown for n = 0, 3, 4, 5, and 6.

Table 5. Observed and Predicted Members of the Homologous Series $RE\mathrm{Zn}_{2-x}\mathrm{As}_2{\cdot}n(RE\mathrm{As})$

			fraction of sites occupied			
n	idealized formula	space group[a]	oct. by RE	tet. by Zn	As stacking	c (Å)
0	$RE\mathrm{Zn}_2\mathrm{As}_2$	$P\bar{3}m1$	1/2	1/2	h (2H)	7.0
1	$RE_2\mathrm{Zn}_2\mathrm{As}_3$[b]	$R\bar{3}m1$	2/3	1/3	h^2c (9R)	10.4 × 3 = 31.2
2	$RE_3\mathrm{Zn}_2\mathrm{As}_4$[b]	$R\bar{3}m1$	3/4	1/4	h^2c^2 (12R)	13.8 × 3 = 41.4
3	$RE_4\mathrm{Zn}_2\mathrm{As}_5$	$P\bar{3}m1$	4/5	1/5	h^2c^3 (5H)	17.2
4	$RE_5\mathrm{Zn}_2\mathrm{As}_6$	$R\bar{3}m1$	5/6	1/6	h^2c^4 (18R)	20.7 × 3 = 62.1
5	$RE_6\mathrm{Zn}_2\mathrm{As}_7$	$R\bar{3}m1$	6/7	1/7	h^2c^5 (21R)	24.2 × 3 = 72.6
6	$RE_7\mathrm{Zn}_2\mathrm{As}_8$	$P\bar{3}m1$	7/8	1/8	h^2c^6 (8H)	27.8
7	$RE_8\mathrm{Zn}_2\mathrm{As}_9$[b]	$R\bar{3}m1$	8/9	1/9	h^2c^7 (27R)	31.2 × 3 = 93.6

[a] Z = 1 ($P\bar{3}m1$) or 3 ($R\bar{3}m1$). [b] Hypothetical compounds.

next member beyond the title compounds, $RE_8\mathrm{Zn}_{2-x}\mathrm{As}_9$ (n = 7), would be expected to have an extremely long c-parameter of nearly 94 Å. A similar structural principle applies to the aluminum carbonitrides $\mathrm{Al}_4\mathrm{C}_3{\cdot}n(\mathrm{AlN})$, in which octahedral and tetrahedral sites are also occupied but the [AlN] slabs added in successive members are of wurtzite-type.[35,36]

The bonding in these arsenides appears simple to rationalize. The average RE–As distances within the [REAs] slabs in these arsenides (La–As, 3.07 Å; Ce–As, 3.04; Pr–As, 3.02 Å; Nd–As, 3.00 Å) are essentially identical to those in the parent rocksalt-type rare-earth monoarsenides REAs themselves (La–As, 3.08 Å; Ce–As, 3.04 Å; Pr–As, 3.01 Å; Nd–As, 2.99 Å).[32,33] The Zn–As distances range from 2.554(2) to 2.603(1) Å, which are similar to those found in the $\mathrm{CaAl}_2\mathrm{Si}_2$-type arsenides $\mathrm{Ce}_{0.629}\mathrm{Zn}_2\mathrm{As}_2$ (2.526(1)–2.624(1) Å)[14] and $\mathrm{YbZn}_2\mathrm{As}_2$ (2.520–2.595 Å).[17] The Zn–Zn distances exceed 3.0 Å, well beyond the sum of the Pauling metallic radii ($2r_{\mathrm{Zn}}$ = 2(1.213 Å) = 2.426 Å),[37] and are likely nonbonding. The As atoms are surrounded by either RE atoms (CN6, octahedral) or by both RE and Zn atoms (CN7, capped octahedral). The absence of both metal–metal and As–As bonding thus implies a reasonable charge assignment with closed shell (RE^{3+}, As^{3-}) or closed subshell (Zn^{2+}) configurations. Such an assignment would lead to excess electrons if the idealized formulation is taken, $(RE^{3+})(\mathrm{Zn}^{2+})_2(\mathrm{As}^{3-})_2\mathrm{e}^-{\cdot}n(RE^{3+}\mathrm{As}^{3-})$. In the parent $\mathrm{CaAl}_2\mathrm{Si}_2$-type phases ($n$ = 0) formed by the early trivalent

dx.doi.org/10.1021/ic400933v | Inorg. Chem. 2013, 52, 7261–7270

RE metals (La–Nd, Sm), removal of this electron excess is manifested as defects in the *RE* sites, $(RE^{3+})_{0.67}(Zn^{2+})_2(As^{3-})_2$.[14] The alternative response is through the formation of Zn defects, giving the charge-balanced formulation $(RE^{3+})(Zn^{2+})_{1.5}(As^{3-})_2 \cdot n(RE^{3+}As^{3-})$. This Zn deficiency is not quite attained in the observed compositions $RE Zn_{1.7-1.8}As_2 \cdot n(REAs)$; a narrow homogeneity range may also be possible, although this remains to be further investigated. Moreover, in one of the structure refinements, there appears a second minor Zn site whose proximity to an As site necessitates partial occupancy in the latter, $Nd_6Zn_{1.65(2)}As_{6.83(1)}$. There is evidence that the rare-earth monoarsenides *RE*As themselves are prone to slight nonstoichiometry in both *RE* and As sites.[33] The characterization of two Mn-substituted derivatives, $Ce_4Mn_{0.6}Zn_{1.2}As_5$ and $Ce_6Mn_{0.4}Zn_{1.3}As_7$, suggests that this formulation is robust and that isostructural compounds can be prepared in which Zn is replaced by other d^0, d^5, or d^{10} substituents. This type of substitution often occurs in other cases, such as the diluted magnetic semiconductors $(Zn_{1-x}Mn_x)_3As_2$[38] and ternary Zintl phases $A_{14}MPn_{11}$.[39] Efforts are in progress to investigate the solid solubility of Mn into $RE Zn_{2-x}As_2 \cdot n(REAs)$ more systematically.

To verify the bonding picture described above, the electronic band structures of these arsenides were analyzed. As a representative example, an idealized $La_4Zn_2As_5$ model with fully occupied Zn sites was first examined (Figure 4). The

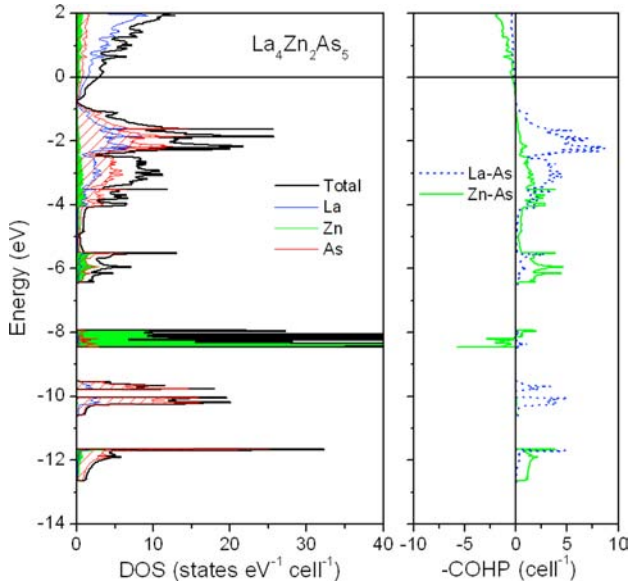

Figure 4. $La_4Zn_2As_5$: The left panel shows the density of states (DOS) and its La (blue line), Zn (filled green region), and As projections (hatched red region); the right panel shows the crystal orbital Hamilton population (COHP) curves for La–As (dotted blue line) and Zn–As interactions (solid green line). The Fermi level is at 0 eV for the idealized nondefect composition $La_4Zn_2As_5$.

density of states (DOS) curve is clearly partitioned into mostly empty La-based bands above the Fermi level (at 0 eV), a broad manifold (−0.8 to −6.5 eV) in which mostly As 4p states mix with La- and Zn-based states, and several low-lying narrow bands corresponding to Zn 3d states (near −8 eV) and As 4s states (near −10 and −12 eV). As deduced from the crystal orbital Hamilton population (COHP) curves, the Zn–As bonding levels lie lower in energy than do the La–As bonding levels, reflecting the stronger covalent bonding character of the former type. The integrated COHP values (−ICOHP) are 0.96 eV/bond for La–As and 1.64 eV/bond for Zn–As bonds. The switch to antibonding character occurs at −0.8 eV, at which point the DOS diminishes to a pseudogap (not quite zero, but nearly so at 0.004 states eV^{-1} $cell^{-1}$). The Fermi level can be lowered to this pseudogap, so that La–As and Zn–As bonding interactions are just optimized, if the electron count is decreased by one (from 61 to 60 e^-/f.u. for the electrons included in the basis set) through the introduction of Zn vacancies. The electrons are assumed to be removed from the higher-energy Zn 4s/4p states which lie closer to the Fermi level than the filled Zn 3d states (which would not be involved in Zn–As bonding). If the configuration of a neutral Zn atom ($4s^2$ $3d^{10}$) is used for the purpose of simplifying the electron counting, removal of one electron over the two Zn atoms in the formula unit would correspond to the formulation $La_4Zn_{1.5}As_5$, in agreement with the argument presented earlier. The observed compositions of this and the other ternary arsenides are closer to $RE Zn_{1.7-1.8}As_2 \cdot n(REAs)$, perhaps because geometrical distortions around the Zn atoms may ensue from vacancy ordering to adjust the energies of bands near the Fermi level. As well, such distortions could lead to strengthened Zn–Zn bonding, which are only negligible (−ICOHP of 0.15 eV/bond) in the idealized $La_4Zn_2As_5$ model. In lieu of Zn deficiencies, it would be interesting to attempt the preparation of fully stoichiometric compounds obtained through substitution of *RE* with a divalent element, such as $SrLa_3Zn_2As_5$, or substitution of Zn with a monovalent element, such as $La_4CuZnAs_5$.

The successive addition of [*RE*As] slabs in the structural evolution of the homologous series $RE Zn_{2-x}As_2 \cdot n(REAs)$ should be paralleled by trends in the electronic structure. The DOS curves for known and missing members of this series in idealized models, as well as for LaAs (rocksalt-type) itself, can be compared (Figure 5). The general features described above for $La_4Zn_2As_5$ are preserved in the DOS curves here, namely, the presence of a valence band based primarily on Zn and As states and a conduction band based on La states. The valence and conduction bands are separated by a band gap of about 0.6 eV in $LaZn_2As_2$, which gradually narrows until these bands just touch in $La_4Zn_2As_5$ so that only a pseudogap remains as further [*RE*As] slabs are inserted. If the DOS curves are decomposed into projections belonging to the [*RE*As] vs $[Zn_2As_2]$ slabs, it can be clearly seen that the band gap narrowing originates from the [*RE*As] slabs, while the states belonging to the $[Zn_2As_2]$ slabs remain relatively unchanged. In all these ternary arsenides, the Fermi level is too high in the idealized formulations, but it can be lowered to precisely the location of the band gap (or pseudogap) by removing one electron per formula unit, which accounts for the Zn substoichiometry as mentioned before. When the extreme case of LaAs is reached in which an infinite number of [*RE*As] slabs and no $[Zn_2As_2]$ slabs are present, the band structure reverts to that of a semimetal, with essentially filled As states and empty La states, in agreement with previous calculations using various methods.[40−43] This analysis demonstrates that the electronic structure of the ternary arsenides can be regarded as a superposition of nearly separate [*RE*As] and $[Zn_2As_2]$ slabs, and that the semiconducting behavior typical of $CaAl_2Si_2$-type phases can be transformed into semimetallic behavior when the number of [*RE*As] slabs introduced exceeds three.

dx.doi.org/10.1021/ic400933v | *Inorg. Chem.* 2013, 52, 7261−7270

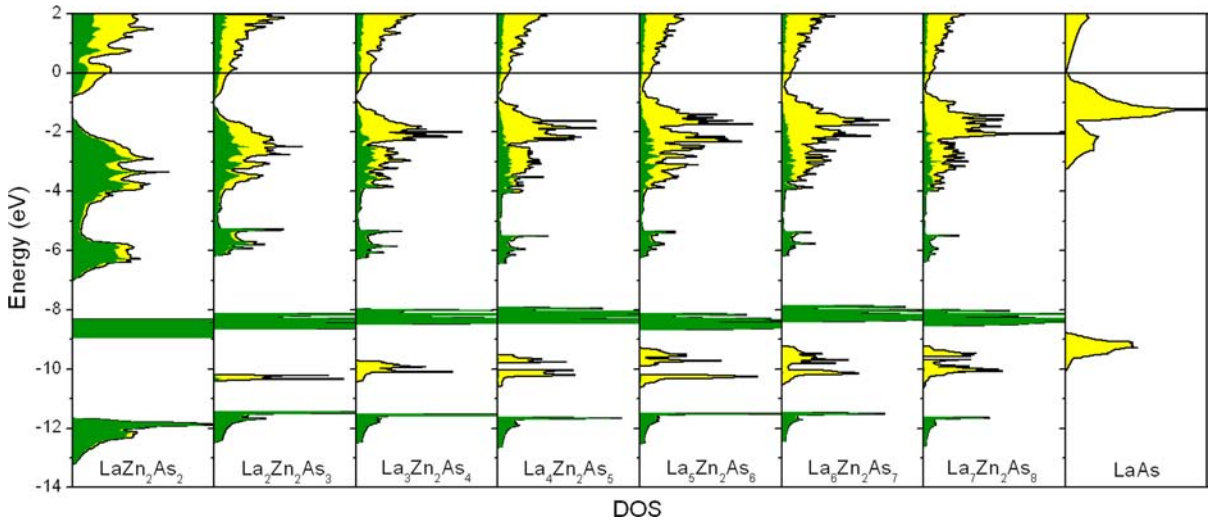

Figure 5. DOS curves for known and hypothetical arsenides with idealized compositions $RE\mathrm{Zn_2As_2}{\cdot}n(RE\mathrm{As})$, and for rocksalt-type NaCl. The DOS curves are decomposed into projections belonging to the $[\mathrm{Zn_2As_2}]$ (green regions) and $[RE\mathrm{As}]$ slabs (yellow regions) that build up the crystal structures of these arsenides.

CONCLUSIONS

The large number of ternary arsenides $RE\mathrm{Zn_{2-x}As_2}{\cdot}n(RE\mathrm{As})$ (RE = La–Nd, Sm; n = 3, 4, 5, 6) presented here demonstrate the effectiveness of a structural principle first identified in a more limited series of phosphides $RE\mathrm{Zn_{2-x}P_2}{\cdot}n(RE\mathrm{P})$ (RE = La, Ce; n = 2, 3, 4).[25−27] We predict that other pnictides can be prepared by applying this principle of alternating $[\mathrm{Zn_2}Pn_2]$ slabs with an increasing number of $[REPn]$ slabs. It is also tempting to suggest that such pnictides would form part of a larger family of infinitely adaptive structures, similar to bismuth chalcogenides (e.g., $(\mathrm{Bi_2})_m(\mathrm{Bi_2Te_3})_n$),[44−47] in which *"every possible composition can attain a unique, fully ordered structure"* through variation of a small number of structural subunits.[28] Thus, we speculate the existence of further ternary rare-earth-containing arsenides in which not only $[RE\mathrm{As}]$ slabs but also $[\mathrm{Zn_2As_2}]$ slabs could be condensed together in an independent fashion to attain any composition, within limits. Although there are examples in which two or three $[\mathrm{Zn_2As_2}]$ slabs are condensed to give tetragonal arrangements (in $\mathrm{RbZn_4As_3}$[48] and $RE\mathrm{Zn_2As_3}$ (RE = La–Pr),[11] respectively), none is currently known in which such slabs are condensed to give trigonal arrangements. However, pairs of $[\mathrm{Cd_2As_2}]$ slabs condensed to give a thicker $[\mathrm{Cd_4As_3}]$ slab in the desired trigonal arrangement are found in $\mathrm{RbCd_4As_3}$.[48] It would thus be worthwhile to seek the formation of infinitely adaptive structures within the RE–Cd–As systems.

The structural flexibility allows the electronic structure to be gradually modified, from semiconducting to semimetallic behavior, as predicted by band structure calculations. In combination with the chemical flexibility provided by the range of RE substitution range and the nonstoichiometry in Zn, it is possible to imagine that considerable control can be exerted on the electrical and magnetic properties of these compounds. Pending efforts to improve sample homogeneity to determine these properties, preliminary magnetic measurements on a few samples ($\mathrm{Ce_5Zn_{2-x}As_6}$, $\mathrm{Pr_6Zn_{2-x}As_7}$, $\mathrm{Nd_7Zn_{2-x}As_8}$) indicate Curie–Weiss behavior with possibly antiferromagnetic ordering.

ASSOCIATED CONTENT

Supporting Information

X-ray crystallographic files in CIF format, EDX analyses, and powder XRD patterns. This material is available free of charge via the Internet at http://pubs.acs.org.

AUTHOR INFORMATION

Corresponding Author

*E-mail: arthur.mar@ualberta.ca.

Notes

The authors declare no competing financial interest.

ACKNOWLEDGMENTS

This work was supported by the Natural Sciences and Engineering Research Council of Canada.

REFERENCES

(1) Mandrus, D.; Sefat, A. S.; McGuire, M. A.; Sales, B. C. *Chem. Mater.* **2010**, *22*, 715–723.
(2) Johrendt, D.; Hosono, H.; Hoffmann, R.-D.; Pöttgen, R. *Z. Kristallogr. - Cryst. Mater.* **2011**, *226*, 435–446.
(3) Johrendt, D. *J. Mater. Chem.* **2011**, *21*, 13726–13736.
(4) Stoyko, S. S.; Blanchard, P. E. R.; Mar, A. *Inorg. Chem.* **2010**, *49*, 2325–2333.
(5) Stoyko, S. S.; Mar, A. *J. Solid State Chem.* **2011**, *184*, 2360–2367.
(6) Stoyko, S. S.; Mar, A. *Inorg. Chem.* **2011**, *50*, 11152–11161.
(7) Stoyko, S. S.; Khatun, M.; Mar, A. *Inorg. Chem.* **2012**, *51*, 2621–2628.
(8) Stoyko, S. S.; Khatun, M.; Mullen, C. S.; Mar, A. *J. Solid State Chem.* **2012**, *192*, 325–330.
(9) Stoyko, S. S.; Khatun, M.; Mar, A. *Inorg. Chem.* **2012**, *51*, 9517–9521.
(10) Stoyko, S. S.; Blanchard, P. E. R.; Mar, A. *J. Solid State Chem.* **2012**, *194*, 113–118.
(11) Lin, X.; Stoyko, S. S.; Mar, A. *J. Solid State Chem.* **2012**, *199*, 189–195.
(12) Khatun, M.; Stoyko, S. S.; Mar, A. *Inorg. Chem.* **2013**, *52*, 3148–3158.
(13) Nientiedt, A. T.; Jeitschko, W. *J. Solid State Chem.* **1999**, *142*, 266–272.
(14) Nientiedt, A. T.; Lincke, H.; Rodewald, U. Ch.; Pöttgen, R.; Jeitschko, W. *Z. Naturforsch. B: J. Chem. Sci.* **2011**, *66*, 221–226.

(15) Klüfers, P.; Neumann, H.; Mewis, A.; Schuster, H.-U. *Z. Naturforsch. B: Anorg. Chem., Org. Chem.* **1980**, *35*, 1317−1318.
(16) Zwiener, G.; Neumann, H.; Schuster, H.-U. *Z. Naturforsch. B: Anorg. Chem., Org. Chem.* **1981**, *36*, 1195−1197.
(17) Nateprov, A.; Cisowski, J.; Heimann, J.; Mirebeau, I. *J. Alloys Compd.* **1999**, *290*, 6−9.
(18) Saparov, B.; Bobev, S. *Acta Crystallogr., Sect. E: Struct. Rep. Online* **2010**, *66*, i24.
(19) Klüfers, P.; Mewis, A. *Z. Kristallogr.* **1984**, *169*, 135−147.
(20) Zheng, C.; Hoffmann, R. *J. Solid State Chem.* **1988**, *72*, 58−71.
(21) Burdett, J. K.; Miller, G. J. *Chem. Mater.* **1990**, *2*, 12−26.
(22) Kranenberg, C.; Johrendt, D.; Mewis, A. *Z. Anorg. Allg. Chem.* **1999**, *625*, 1787−1793.
(23) Stoyko, S. S.; Mar, A. unpublished information.
(24) Frik, L.; Mewis, A. *Z. Anorg. Allg. Chem.* **1999**, *625*, 126−130.
(25) Lincke, H.; Nilges, T.; Johrendt, D.; Pöttgen, R. *Solid State Sci.* **2008**, *10*, 1006−1011.
(26) Lincke, H.; Hermes, W.; Nilges, T.; Pöttgen, R. *Solid State Sci.* **2008**, *10*, 1480−1484.
(27) Lincke, H.; Nilges, T.; Pöttgen, R. *Z. Anorg. Allg. Chem.* **2008**, *634*, 2885−2888.
(28) Anderson, J. S. *J. Chem. Soc., Dalton Trans.* **1973**, 1107−1115.
(29) Sheldrick, G. M. *SHELXTL*, version 6.12; Bruker AXS Inc.: Madison, WI, 2001.
(30) Gelato, L. M.; Parthé, E. *J. Appl. Crystallogr.* **1987**, *20*, 139−143.
(31) Tank, R.; Jepsen, O.; Burkhardt, A.; Andersen, O. K. *TB-LMTO-ASA Program*, version 4.7; Max Planck Institut für Festkörperforschung: Stuttgart, Germany, 1998.
(32) Brixner, L. H. *J. Inorg. Nucl. Chem.* **1960**, *15*, 199−201.
(33) Taylor, J. B.; Calvert, L. D.; Despault, J. G.; Gabe, E. J.; Murray, J. J. *J. Less-Common Met.* **1974**, *37*, 217−232.
(34) Pearson, W. B. *The Crystal Chemistry and Physics of Metals and Alloys*; Wiley: New York, 1972.
(35) Jeffrey, G. A.; Wu, V. Y. *Acta Crystallogr.* **1963**, *16*, 559−566.
(36) Jeffrey, G. A.; Wu, V. Y. *Acta Crystallogr.* **1966**, *20*, 538−547.
(37) Pauling, L. *The Nature of the Chemical Bond*, 3rd ed.; Cornell University Press: Ithaca, NY, 1960.
(38) Denissen, C. J. M.; Sun, D. K.; Kopinga, K.; de Jonge, W. J. M.; Nishihara, H.; Sakakibara, T.; Goto, T. *Phys. Rev. B* **1987**, *36*, 5316−5325.
(39) Kauzlarich, S. M. In *Chemistry, Structure, and Bonding of Zintl Phases and Ions*; Kauzlarich, S. M., Ed.; VCH Publishers: New York, 1996; pp 245−274.
(40) Hasegawa, A. *J. Phys. C: Solid State Phys.* **1980**, *13*, 6147−6156.
(41) Deligöz, E.; Çolakoğlu, K.; Çiftçi, Y. Ö.; Özişik, H. *J. Phys.: Condens. Matter* **2007**, *19*, 436204−1−436204−11.
(42) Uğur, G.; Uğur, Ş.; Erkişi, A.; Soyalp, F. *Int. J. Mod. Phys. B* **2008**, *22*, 5027−5033.
(43) Charifi, Z.; Reshak, A. H.; Baaziz, H. *Solid State Commun.* **2008**, *148*, 139−144.
(44) Lind, H.; Lidin, S. *Solid State Sci.* **2003**, *5*, 47−57.
(45) Bos, J. W. G.; Zandbergen, H. W.; Lee, M.-H.; Ong, N. P.; Cava, R. J. *Phys. Rev. B* **2007**, *75*, 195203−1−195203−9.
(46) Bos, J.-W. G.; Faucheux, F.; Downie, R. A.; Marcinkova, A. *J. Solid State Chem.* **2012**, *193*, 13−18.
(47) Valla, T.; Ji, H.; Schoop, L. M.; Weber, A. P.; Pan, Z.-H.; Sadowski, J. T.; Vescovo, E.; Fedorov, A. V.; Caruso, A. N.; Gibson, Q. D.; Müchler, L.; Felser, C.; Cava, R. J. *Phys. Rev. B* **2012**, *86*, 241101-1−241101-5.
(48) He, H.; Tyson, C.; Bobev, S. *Inorg. Chem.* **2011**, *50*, 8375−8383.